Numerical Simulation of the Effects of Charge Stratification on Combustion and Emissions

Zhaolei Zheng and Mingfa Yao*

State Key Laboratory of Engines, Tianjin University, Tianjin, 300072, China

Received February 7, 2007. Revised Manuscript Received April 18, 2007

A fully coupled multidimensional computational fluid mechanics and reduced chemical kinetics model is adopted to investigate the effects of charge stratification on combustion and emissions. Seven different kinds of imposed stratification have been introduced according to the position of the maximal local fuel/air equivalence ratio in the cylinder at intake valve close. The results show that the charge stratification results in stratification of the in-cylinder temperature. The former four kinds of stratification, whose maximal local equivalence ratios locate between the cylinder center and half of the cylinder radius, advance ignition timing, reduce the pressure-rise rate, and retard combustion phasing. But the following three kinds of stratification, whose maximal local equivalence ratios appear between half of the cylinder radius and the cylinder wall, have little effect on the cylinder pressure. For the two discussed equivalence ratios, all kinds of stratification can reduce unburned fuel emissions; all kinds of stratification can reduce formaldehyde emissions when the mixture is lean, and only the last two kinds of stratification can reduce formaldehyde emissions when the mixture is comparatively rich; the former four kinds of stratification deteriorate the CO and NOx emissions, and the last two kinds of stratification can reduce unburned fuel, formaldehyde, and CO emissions and maintain low NOx emissions simultaneously.

1. Introduction

Homogeneous charge compression ignition (HCCI) remains an area of interest due to its potential in significantly reducing NOx and particulate emissions, while achieving high thermal efficiency at part load.[1−3] Therefore, HCCI is considered as a high-efficiency alternative to spark-ignited gasoline operation and a low-emissions alternative to traditional diesel compression ignition combustion. However, several technical barriers must be overcome before HCCI can be implemented in production engines. HCCI engines tend to have high unburned hydrocarbon (UHC) and carbon monoxide (CO) emissions, high rates of heat release, and high peak cylinder pressures.

A large number of groups have ongoing research efforts in exploring and understanding the design, operation, and control of HCCI engines.[4−6] Much of the previous experimental work related to the HCCI engine process has been directed under conditions of homogeneous in-cylinder temperature and composition, most commonly achieved using early premixing or port fuel injection strategies with careful temperature management. Solving the HCCI control problems has led to the investigation of various control strategies that may move away from truly homogeneous mixtures, including direct injection[7] and variable valve actuation.[8,9] With HCCI, the start of combustion is indicated by autoignition chemical kinetics. Thus, controlling the combustion phasing requires tuning the autoignition kinetics, which is affected by the charge composition and the pressure and temperature histories of the reactants during the compression process. Therefore, stratification methods which may result in a mixture with significant composition and temperature stratification, while retaining chemical-kinetics-dominated ignition, may be desirable in controlling HCCI combustion.

The role of inherent thermal stratification from heat transfer and its effect on HCCI operation were considered in terms of combustion and emissions by Aceves and his co-workers[10] using a simplified multizone model to capture boundary layer and crevice effects. Recent and forthcoming research by Dec and Sjöberg[11] and Sjöberg and co-workers[12,13] included both engine experiments and multizone numerical models. They demonstrate that thermal stratification including temperature gradients and

* Corresponding author. Tel.: 86-22-27406842 ext. 8014. Fax: 86-22-27383362. E-mail: y_mingfa@tju.edu.cn

(1) Onishi, S.; Jo, S. H.; Shoda, K.; Jo, P. D.; Kato, S. Active Thermo-Atmosphere Combustion: A New Combustion Progress for Internal Combustion Engines. *SAE Tech. Pap. Ser.* **1979**, 790501.

(2) Thring, R. H. Homogeneous-Charge Compression Ignition (HCCI) Engines. *SAE Tech. Pap. Ser.* **1989**, 892068.

(3) Lshibashi, Y. Basic Understanding of Activated Radical Combustion and Its Two-Stroke Engine Application and Benefits. *SAE Tech. Pap. Ser.* **2000**, 2000-01-1836.

(4) Yao, M. F.; Zheng, Z. Q.; Qin, J. Experimental Study on HCCI Combustion with Fuel of Dimethyl Ether and Natural Gas. *J. Eng. Gas Turbines Power* **2006**, *128*, 414−420.

(5) Yao, M. F.; Chen, Z.; Zheng, Z. Q. Study on the Controlling Strategies of Homogeneous Charge Compression Ignition Combustion with Fuel of Dimethyl Ether and Methanol. *Fuel* **2006**, *85*, 2046−2056.

(6) Kong, S. C.; Marriot, C. D.; Reitz, R. D.; Christensen, M. Modeling and Experiments of HCCI Engine Combustion Using Detailed Chemical Kinetics With Multidimensional CFD. *SAE Tech. Pap. Ser.* **2001**, 2001-01-1026.

(7) Marriot, C. D.; Reitz, R. D. Experimental Investigation of Direct Injection-Gasoline for Premixed Compression Ignited Combustion Phasing Control. *SAE Tech. Pap. Ser.* **2002**, 2002-01-0418.

(8) Kaahaaina, N. B.; Simon, A. J.; Caton, P. A.; Edwards, C. F. Use of Dynamic Valving to Achieve Residual-Affected Combustion. *SAE Tech. Pap. Ser.* **2001**, 2001-01-0549.

(9) Law, D.; Kemp, D.; Allen, J.; Kirkpatrick, G.; Copland, T. Controlled Combustion in an IC-Engine with a Fully Variable Valve Train. *SAE Tech. Pap. Ser.* **2001**, 2001−01−0251.

(10) Aceves, S.; Flowers, D.; Westbrook, C.; Smith, R.; Dibble, R.; Christensen, M.; Pitz, W.; Johansson, B. A Multi-Zone Model for Prediction of HCCI Combustion and Emissions. *SAE Tech. Pap. Ser.* **2000**, 2000-01-0327.

10.1021/ef070071k CCC: $37.00
Published on Web 05/31/2007

composition gradients is one approach to achieve high speed and high load. Model results also indicated the potential of thermal stratification to reduce the peak heat release rate. Reference 11 shows that the naturally occurring thermal stratification caused by heat transfer can be influenced by techniques such as changing the coolant temperature and air swirl. This work convincingly illustrates the potential of the thermal design control using achievable temperature distributions. But for thermal stratification, it is unclear how a controlled thermal stratification would best be generated for a practical engine, while minimizing heat-transfer losses and cycle-to-cycle variations. Nonetheless, this can be considered a promising area of HCCI research, and there are considerable amounts of research activities in related areas.[14−19]

With homogeneous charge, 10% of the fuel can exit the cylinder unburned.[18] Consequently, one could assume that this amount of fuel does not contribute to the pressure rise. If one imagines that all of the fuel was supplied via direct injection to the cylinder with less fuel in the quenching zones, the operational equivalence ratio in the combustion zone would rise relative to the homogeneous charge operation. Thus, it would be possible to reduce the amount of fuel residing in the quenching zones using charge stratification. Consequently, the fuel economy could be improved and the HCCI operating range can be expanded. Richter and co-workers[20] performed engine imaging experiments to assess the magnitude and role of inhomogeneities in HCCI operation. They concluded that charge inhomogeneities were potentially significant and played an important role in the combustion process. The results also demonstrated that the natural inhomogeneities were present even for effectively premixed charges. Noda and Foster[21] utilized a hydrogen-fueled numerical model to infer inhomogeneities to be necessary to recover quantitative combustion durations. Aceves and co-workers[22] have considered the role of fuel structure and equivalence ratio in extending combustion duration and controlling combustion phasing. Related research has been presented by several research groups.[19,23−24] Furthermore, the diesel industry has extensive experience with direct fuel injection and advanced charge preparation techniques. Techniques have been developed that can help the utilization of needed premixed combustion modes.[25−27] Mixture stratification modifies local equivalence ratios and has been suggested as a potential mechanism for controlling HCCI combustion.

Detailed chemical kinetics are usually used to simulate HCCI combustion. Much research has been implemented on the HCCI combustion process with different fuels using elementary reactions.[28−30] Iida and Sato revealed the low-temperature reaction, high-temperature reaction, and emissions mechanisms of hydrocarbon fuels (such as N-butane)[28] and oxygenated fuels (such as dimethyl ether).[29] Daisho and colleagues revealed the effects of initial charge conditions, compression ratio, and excess air ratio on ignition and combustion and HCCI regions of an *n*-heptane/air mixture.[30] However, using chemical kinetics alone has not been successful to simulate the combustion by assuming a uniform temperature distribution, that is, the so-called single-zone model. The in-cylinder temperature is actually nonuniform, and the high-temperature region in the center of the chamber is more responsible for the ignition. In theory, any engine combustion problem could be solved by linking a fluid mechanics code with a chemical kinetics code including HCCI combustion and charge stratification combustion where partial composition stratification exists. Multidimensional computational fluid mechanics (CFD) models coupled directly with chemical kinetics can analyze effects of the nonuniformities on autoignition and combustion, and they can also analyze effects of the in-cylinder turbulence on combustion. Daisho and Kusaka developed a multidimensional model combined with a detailed kinetics by the link between KIVA-3 and CHEMKIN-II with some modifications to investigate the chemical reaction phenomena encountered in the HCCI combustion process of natural gas.[31] Kong et al. used modified KIVA code along with

(11) Dec, J. E.; Sjöberg, M. Isolating the Effects of Fuel Chemistry on Combustion Phasing in an HCCI Engine and the Potential of Fuel Stratification for Ignition Control. *SAE Tech. Pap. Ser.* **2004**, 2004-01-0557.

(12) Sjöberg, M.; Dec, J. E.; Cernansky, N. P. Potential of Thermal Stratification and Combustion Retard for Reducing Pressure-Rise Rates in HCCI Engines, Based on Multi-Zone Modeling and Experiments. *SAE Tech. Pap. Ser.* **2005**, 2005-01-0113.

(13) Sjöberg, M.; Dec, J. E. Effects of Engine Speed, Fueling Rate, and Combustion Phasing on the Thermal Stratification Required to Limit HCCI Knocking Intensity. *SAE Tech. Pap. Ser.* **2005**, 2005-01-2125.

(14) Amano, T.; Morimoto, S.; Kawabata, Y. Modeling of the Effect of Air/Fuel Ratio and Temperature Distribution on HCCI Engines. *SAE Tech. Pap. Ser.* **2001**, 2001-01-1024.

(15) Noda, T.; Foster, D. E. A Numerical Study to Control Combustion Duration of Hydrogen-Fueled HCCI by Using Multi-Zone Chemical Kinetics Simulation. *SAE Tech. Pap. Ser.* **2001**, 2001-01-0250.

(16) Babajimopoulos, A.; Lavoie, G. A.; Assanis, D. N. Modeling HCCI Combustion with High Levels of Residual Gas Fraction − A Comparison of Two VVA Strategies. *SAE Tech. Pap. Ser.* **2003**, 2003-01-3220.

(17) Grenda, J. M. Numerical Modeling of Charge Stratification for the Combustion Control of HCCI Engines. *SAE Tech. Pap. Ser.* **2005**, 2005-01-3722.

(18) Schiessl, R.; Maas, U. Analysis of Endgas Temperature Fluctuations in an SI Engine by Laser-induced Fluorescence. *Combust. Flame* **2003**, *133*, 19−27.

(19) Sankaran, R.; Im, H. G. Effects of Mixture Inhomogeneity on the Auto-Ignition of Reactants under HCCI Environment. *AIAA Pap.* **2004**, 2004-1328.

(20) Richter, M.; Engström, J.; Franke, A.; Aldén, M.; Hultqvist, A.; Johansson, B. The Influence of Charge Inhomogeneity on the HCCI Combustion Process. *SAE Tech. Pap. Ser.* **2000**, 2000-01-2868.

(21) Noda, T.; Foster, D. A Numerical Study to Control Combustion Duration of Hydrogen-Fueled HCCI Using Multi-Zone Chemical Kinetics Simulations. *SAE Tech. Pap. Ser.* **2001**, 2001-01-0250.

(22) Aceves, S.; Flowers, D. L.; Espinosa-Loza, F.; Babajimopoulos, A.; Assanis, D. N. Analysis of Premixed Charge Compression Ignition Combustion with a Sequential Fluid Mechanics-Multizone Chemical Kinetics Model. *SAE Tech. Pap. Ser.* **2005**, 2005-01-0115.

(23) Bradley, D.; Morley, C.; Gu, X. J.; Emerson, D. Amplified Pressure Waves During Autoignition: Relevance to CAI Engines. *SAE Tech. Pap. Ser.* **2002**, 2002-01-2868.

(24) Xu, H.; Liu, M.; Gharahbaghi, S.; Richardson, S.; Wyszynski, M.; Megaritis, T. Modeling of HCCI Engines: Comparison of Single-Zone, Multi-Zone, and Test Data. *SAE Tech. Pap. Ser.* **2005**, 2005-01-2123.

(25) Duret, P.; Gatellier, B.; Monteiro, L.; Miche, M.; Zima, P.; Maroteaux, D.; Guezet, J.; Blundell, D.; Spinnler, F.; Zhao, H.; Perotti, M.; Araeo, L. Process in Diesel HCCI Combustion Within the European Space Light Project. *SAE Tech. Pap. Ser.* **2004**, 2004-01-1904.

(26) Hergart, C.-A.; Barths, H.; Siewert, R. M. Modeling Approaches for Partially Premixed Compression Ignition Combustion. *SAE Tech. Pap. Ser.* **2005**, 2005-01-0218.

(27) Wåhlin, F.; Cronhjort, A.; Olofsson, U.; Ångström H.-E. Effect of Injection Pressure and Engine Speed on Air/Fuel Mixing and Emissions in a Pre-Mixed Compression-Ignited (PCI) Engine Using Diesel Fuel. *SAE Tech. Pap. Ser.* **2004**, 2004-01-2989.

(28) Sato, S.; Iida, N. Analysis of DME Homogenous Charge Compression Ignition. Combustion. *SAE Tech. Pap. Ser.* **2003**, 2003-01-1825.

(29) Yamasaki, Y.; Iida, N. Numerical Analysis of Auto Ignition and Comubstion of n-Butane and Air Mixture in the Homogeneous Charge Compression Ignition Engine by Using Elementary Reactions. *SAE Tech. Pap. Ser.* **2003**, 2003-01-1090.

(30) Kusaka, J.; Yamamoto, T.; Daisho, Y. Simulating the Homogeneous Charge Compression Ignition Process Using a Detailed Kinetics Model for n-Heptane Mixture. *Int. J. Engine Res.* **2001**, *1*, 281−89.

(31) Kusaka, J.; Daisho, Y. Multi-Dimensional Modeling Combined with a Detailed Kinetics (Application for HCCI of Natural Gas). The Fifth International Symposium on Diagnostics and Modeling of Combustion in Internal Combustion Engines, Nagoya, Japan, Jul. 1−4, 2001; *Proceedings of 5th COMODIA*; The Japan Society of Automotive Engineers: Yokyo, Japan, 2001; pp 330−336.

Table 1. Species and Reactions of *n*-Heptane Reduced Mechanism

NC_7H_{16} O_2 C_7H_{15}-3 HO_2 $C_7H_{15}O_2$-3 $C_7H_{14}OOH3-5$ $C_7H_{14}OOH3$-$5O_2$ NC_7KET35 OH C_2H_5CHO H_2O $C_2H_5COCH_2$ CH_2O C_4H_8-1 H_2O_2 NC_3H_7 C_2H_3 CH_3O C_2H_5 H HCO O CO CO_2 CH_3 C_2H_4 N_2 C_2H_5CO C_2H_5O CH_2CO C_4H_7 C_4H_6 C_4H_7O CH_3CHO CH_3CO

1. $NC_7H_{16} + OH = C_7H_{15}$-3 $+ H_2O$
2. $NC_7H_{16} + HO_2 = C_7H_{15}$-3 $+ H_2O_2$
3. $NC_7H_{16} + O_2 = C_7H_{15}$-3 $+ HO_2$
4. $C_7H_{15}O_2$-3 $= C_7H_{15}$-3 $+ O_2$
5. $C_7H_{15}O_2$-3 $= C_7H_{14}OOH3$-5
6. $C_7H_{14}OOH3$-$5O_2 = C_7H_{14}OOH3$-5 $+ O_2$
7. $C_7H_{14}OOH3$-$5O_2 = NC_7KET35 + OH$
8. $NC_7KET35 = C_2H_5CHO + C_2H_5COCH_2 + OH$
9. $C_7H_{14}OOH3$-5 $= OH + C_2H_5CHO + C_4H_8$-1
10. C_7H_{15}-3 $= C_4H_8$-1 $+ NC_3H_7$
11. $H_2O_2 + OH = H_2O + HO_2$
12. $H_2O_2 + O_2 = HO_2 + HO_2$
13. $OH + OH(+M) = H_2O_2(+M)$
14. $H_2O_2 + O_2 = HO_2 + HO_2$
15. $H + O_2 = O + OH$
16. $O + H_2O = OH + OH$
17. $C_2H_3 + O_2 = CH_2O + HCO$
18. $CH_2O + OH = HCO + H_2O$
19. $HCO + M = H + CO + M$
20. $HCO + O_2 = CO + HO_2$
21. $CO + OH = CO_2 + H$
22. $C_2H_5 + O_2 = C_2H_4 + HO_2$
23. $C_2H_4 + OH = C_2H_3 + H_2O$
24. $C_2H_5CO = C_2H_5 + CO$
25. $C_2H_5CHO + OH = C_2H_5CO + H_2O$
26. $C_2H_5 + HO_2 = C_2H_5O + OH$
27. $C_2H_5O = CH_3 + CH_2O$
28. $C_2H_5COCH_2 = CH_2CO + C_2H_5$
29. C_4H_8-1$+OH = C_4H_7 + H_2O$
30. $C_4H_7 + O_2 = C_4H_6 + HO_2$
31. $C_4H_7 + HO_2 = C_4H_7O + OH$
32. $C_4H_6 + OH = C_2H_5 + CH_2CO$
33. $CH_2CO + OH = CH_2O + HCO$
34. $C_4H_7O = CH_3CHO + C_2H_3$
35. $CH_3CHO + OH = CH_3CO + H_2O$
36. $CH_3CO + M = CH_3 + CO + M$
37. $HO_2 + M = H + O_2 + M$
38. $CH_3 + O_2 = CH_3O + O$
39. $CH_3O + O_2 = CH_2O + HO_2$
40. $CH_2O + HO_2 = HCO + H_2O_2$
41. $NC_3H_7 = CH_3 + C_2H_4$

CHEMKIN to study the effects of geometry-generated turbulence on HCCI combustion.[32]

In the current study, *n*-heptane (*n*-C_7H_{16}) is selected as fuel, which has a cetane index of 56, equivalent to that of a diesel fuel. A fully coupled multidimensional CFD code (Star-CD/Kinetics) and chemical kinetics code was used to investigate charge stratification combustion. For *n*-heptane, detailed chemical kinetic (thousands of reactions and hundreds of species) calculations coupled with CFD simulations of chemically reacting flows are still unrealistic as the basis for a parametric simulation tool due to taking large amounts of CPU time. Therefore, a reduced mechanism is adopted. The analysis focuses on how stratification affects ignition, combustion, and emissions, which has significant meaning in demonstrating the potential of charge stratification on overcoming the barriers of HCCI combustion.

2. Computational Model

2.1. Fully Coupled CFD and Chemical Kinetics Model. An *n*-heptane reduced mechanism consisting of 35 species and 41 reactions was used to simulate the fuel chemistry. All species and reactions are showed in Table 1. The mechanism has been validated on the ignition delay and mole fractions of important intermediate species under various conditions that include the range of interest in engine applications by comparison to the results from detailed mechanisms.[33] The mechanism has been implemented in the STAR-CD/KINETICS CFD code to simulate the combustion with an inhomogeneous charge. The STAR-CD code provides CHEMKIN the species and thermodynamic information of the computational cells, and the CHEMKIN code returns the new species information and energy release after solving the chemistry. The chemistry and flow solutions are then coupled.

The RNG$^{k-\epsilon}$ model was used for turbulence modeling. The PISO algorithm was used for the transient flow of the engine. PISO performs at each time (or iteration) step; a predictor is used, followed by a number of correctors, during which linear equation sets are solved iteratively for each main dependent variable. The decisions on the number of correctors and inner iterations are made internally on the basis of the splitting error and inner residual levels, respectively, according to prescribed tolerances and upper limits. On the basis of the finite volume method, the flow domain is discretized into several homogeneous zones (cells). At each cell, the complex chemical kinetics during the HCCI combustion are dealt with using the built-in CHEMKIN module. After the solutions for all cells, the mass transfer, heat transfer between cells, and flow are simulated by the corresponding submodels. Then, the interaction between turbulent mixing and chemical reaction is implemented.

To reduce the computational time, two-dimensional meshes were used as shown in Figure 1. The multidimensional computations started at intake valve close (IVC) and ended at exhaust valve open. The computational time step was a 0.1° crank angle.

2.2. Comparisons of Pressure Profiles and Important Intermediate Species of the Experiment with Calculation. The HCCI experiment was conducted on a single-cylinder, water-cooled, direct-injection diesel engine. Engine specifications are given in Table 2. Figure 2 shows the comparison between the measured in-cylinder pressure profile and the computed result. It can be seen that the computed result agrees well with the measured result.

The CH_2O molecule is formed as an intermediate species during hydrocarbons oxidation. CH_2O is formed in the low-temperature oxidation in the early phase of the ignition process and consumed later in the combustion process. Hence, CH_2O is an indicator of the first stage of ignition and a marker for the low-temperature reactions zones. The OH radical is an important intermediate species that is formed during the combustion. OH is formed in the flame region with high temperatures and often used as a marker of both flame fronts and burnt regions. In ref 34, the images of OH and CH_2O are investigated using laser-induced fluorescence in a single-cylinder HCCI optical engine with a port-fuel injection system. In order to check the validation of the coupled multidimensional CFD and reduced chemical kinetics model, the images of OH and CH_2O are calculated under the same conditions as the experimental conditions in ref 34. Figure 3 shows the comparison of CH_2O and

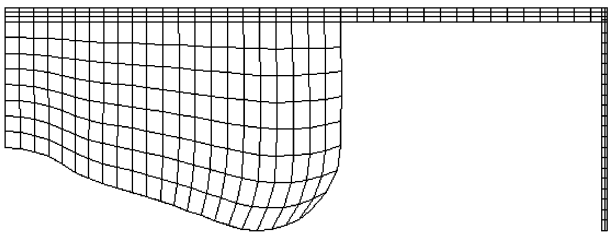

Figure 1. Engine combustion chamber geometry and computational mesh.

(32) Kong, S. C.; Reitz, R. D.; Christensen, M.; Johansson, B. Modeling the Effects of Geometry Generated Turbulence on HCCI Engine Combustion. *SAE Tech. Pap. Ser.* **2003**, 2003-01-1088.

(33) Yao, M. F.; Zheng, Z. L. An Investigation on a New Reduced Chemical Kinetic Model of n-Heptane for HCCI Combustion. *Proc. Inst. Mech. Eng.* **2006**, *220* (D7), 991−1002.

Table 2. Engine Specifications

bore	115 mm
stroke	115 mm
displacement	1200 cm^3
compression ratio	17.0:1
engine speed	1400 r/min
intake valve open	12° BTDC
intake valve close	45° ABDC
exhaust valve open	55° BBDC
exhaust valve close	14° ATDC

OH between simulation and experimentation. The results show that the trends of the calculated and experimental CH_2O and OH images are accordant. Figure 3 also indicates that OH and CH_2O are two different and complementary markers of the combustion process in the HCCI engine. The formation of CH_2O is correlated with the beginning of the cool flame heat release, and the disappearance of CH_2O corresponds to the beginning of the high-temperature reaction. Three peaks of OH radicals are correlated to the low-temperature reaction and two stages of the high-temperature reaction, respectively.

2.3. Initial Conditions. To study the effects of charge stratification, a theoretical stratification is imposed on the fuel and air mixture. Except for this imposed stratification, all conditions are the same among the cases: overall fuel/air ratio, intake temperature and pressure, wall temperature, and so forth. This approach has the disadvantage that the inhomogeneous results cannot be directly compared to the experiment. However, it gives us the ability to directly compare cases in which the only difference is the homogeneous and inhomogeneous nature of the fuel/air mixture.

In the current study, the meshes are divided into 13 layers along the radial direction. The equivalence fuel/air ratio distribution of the 13 layers at IVC is according to function 1.

$$\phi_n = \begin{cases} 0.9\phi_n - 1 & (n > m) \\ 1.1\phi_n - 1 & (n \le m) \end{cases} \quad (1)$$

where m denotes the mesh layer where the maximal local equivalence ratio appears ($1 \le m \le 13$), and ϕ_n represents the equivalence fuel/air ratio of every layer ($n \ge 2$). If m is comparatively large, the fuel concentration distributions are very high near the cylinder liner wall and in the piston-ring crevice regions, which does not accord with the operation conditions of a practical engine. Therefore, the equivalence ratio at the cylinder wall is assumed as 0 when m is larger than 9.

The simulation is done at two overall equivalence ratios of 0.2 and 0.264, which represent a leaner mixture and a comparatively richer mixture in HCCI combustion. Furthermore, seven cases and the uniform fuel/air distribution are calculated at every overall equivalence ratio. The initial equivalence ratio distributions are shown in Table 3. According to the above assumption, the initial equivalence ratios at the cylinder wall given by cases 6 and 7 are 0.

3. Results and Discussion

3.1. Effects of Charge Stratification on Average In-Cylinder Pressure. For HCCI combustion, the chemical reactions occur very fast during the main stage of combustion, which leads to a high pressure-rise rate and short combustion duration. Figure 4 shows the comparison of in-cylinder pressure profiles for all cases at the two overall equivalence ratios. It can be seen that cases 5−7 whose maximal local equivalence ratios appear between half of the cylinder radius and the cylinder wall ($0.5 < r/r_0 < 1$) have no obvious effects on the average in-cylinder pressure compared with the uniform case. On the contrary, cases 1−4 whose maximal equivalence ratios appear between the cylinder centerline and half of the cylinder radius ($0 < r/r_0 < 0.5$) have obvious effects on the average in-cylinder pressure. The pressure profiles from these cases are approximately superposed; moreover, all of them can advance the ignition timing and reduce the pressure-rise rate. The following analysis gives the reason of these results. Cases 1 and 5 with an overall equivalence ratio of 0.264 are selected as representatives to analyze the effects of stratification on the in-cylinder pressure here.

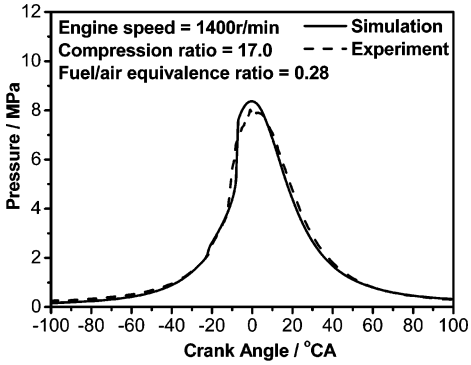

Figure 2. Comparison of cylinder pressure between simulation and experiment.

Figure 5 shows the average in-cylinder temperature distributions of three cases (case 1, case 5, and the uniform case) when the high-temperature reactions are occurring (13° before top dead center, BTDC, for case 5 and the uniform case; 15° BTDC for case 1). For case 5 and the uniform case, the average in-cylinder temperature distributions are almost homogeneous at 13° BTDC, except for the piston-ring crevice regions. While, for case 1, local high-temperature regions exist obviously in the local high equivalence ratio regions at 15° BTDC. According to previous studies, it is well know that the high-temperature reaction of HCCI combustion is mainly dominated by the oxidation process of CH_2O to CO_2. Figure 6 shows the CH_2O concentration distributions in the cylinder from the three cases mentioned above when the high-temperature reactions are occurring. It can be seen that the CH_2O concentration distribution is very homogeneous except for the piston-ring crevice regions for the uniform case, and stratification exists for cases 1 and 5. While, compared with parts b and c of Figure 6, the stratification degree of case 5 is much lower than that of case 1. From the above analysis for Figures 5 and 6, it can be stated that it is because of comparative uniformity of the in-cylinder temperature distribution and CH_2O concentration distribution for case 5 that the in-cylinder pressure profiles given by case 5 are similar to those given by the uniform case. For case 1, local high-temperature and CH_2O concentration regions advance the ignition timing. In addition, low-temperature and CH_2O concentration regions which are larger than local high regions lead to the slowness of the combustion and the reduction of the pressure-rise rate.

Figures 7 and 8 show the average in-cylinder temperature distributions and the CH_2O concentration distributions for all cases at an overall equivalence ratio of 0.264 when the high-temperature reactions are occurring. It can be seen that the former four kinds of stratification combustion have greater temperature gradients and CH_2O concentration gradients than the following three kinds of stratification combustion. Figure 7 indicates that the initial distribution of equivalence ratio has little effect on in-cylinder temperature distribution with the increase of r/r_0 for cases 1−4. When it just exceeds 0.5 (case 5), the in-cylinder temperature is almost uniform except for strong heat-transfer regions. If r/r_0 continues to increase, the stratification degree of the in-cylinder temperature begins to increase slightly (cases 6 and 7), but it is much lower than that

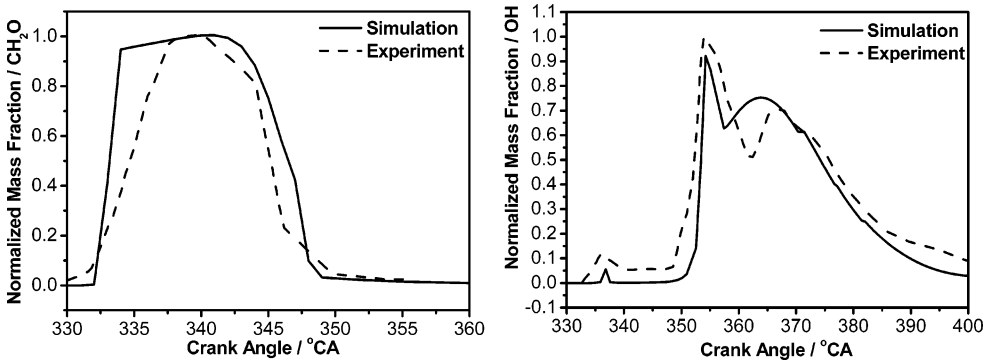

Figure 3. Comparison of CH_2O and OH between simulation and experiment.

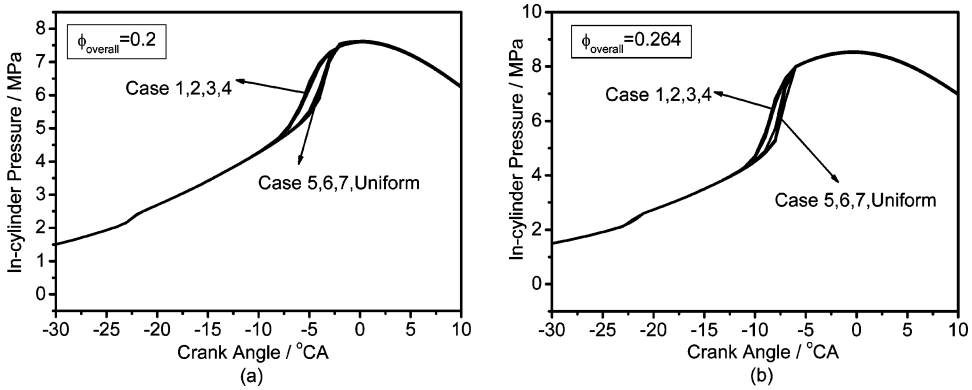

Figure 4. Comparison of pressure for every case at two overall equivalence ratios.

Table 3. Imposed Initial Charge Stratification at the Two Equivalence Ratios[a]

Case	1 (m=1)	2 (m=3)	3 (m=5)	4 (m=7)	5 (m=9)	6 (m=11)	7 (m=13)	Uniform
r/r_0	0	0.14	0.29	0.45	0.61	0.78	0.94	
initial equivalence ratio distributions	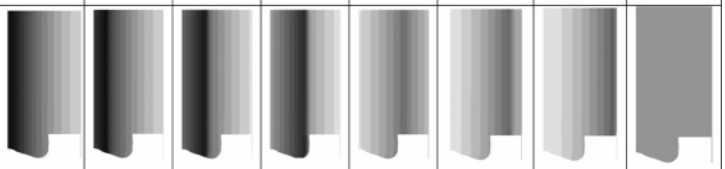							
Scale	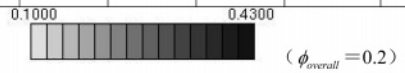 0.1000 0.4300 ($\phi_{overall}$=0.2)							
Case	1 (m=1)	2 (m=3)	3 (m=5)	4 (m=7)	5 (m=9)	6 (m=11)	7 (m=13)	Uniform
r/r_0	0	0.14	0.29	0.45	0.61	0.78	0.94	
initial equivalence ratio distributions	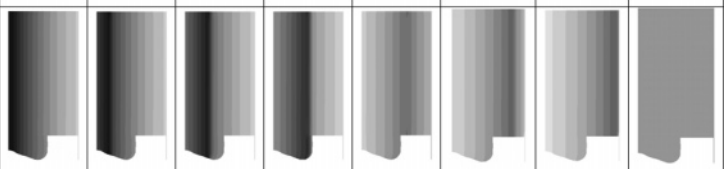							
Scale	 0.1000 0.5800 ($\phi_{overall}$=0.264)							

[a] r_0 indicates the radius of the cylinder; r indicates the distance between the cylinder centerline and the position where the maximal equivalence ratio appears.

of the former four cases. Similarly, Figure 8 indicates that the initial distribution of the equivalence ratio has little effect on CH_2O concentration distribution with the increase of r/r_0 for cases 1−4. However, when r/r_0 is close to 0.5 (case 4), the local CH_2O concentration maximum decreases and the CH_2O concentration gradient becomes small. For the following three cases, When it just exceeds 0.5 (case 5), the stratification degree of CH_2O concentration is the lowest in all cases. If r/r_0 continues to increase, the stratification degree of CH_2O concentration begins to increase slightly (cases 6 and 7), but it is much lower than that of the former four cases.

3.2. Effects of Charge Stratification on Emissions. It is well-known that HCCI combustion can realize very low NOx and particulate matter (PM) emissions but has high UHC and

Figure 5. In-cylinder temperature distributions of the uniform case, case 1, and case 5 when the high-temperature reactions are occurring ($\phi_{overall} = 0.264$).

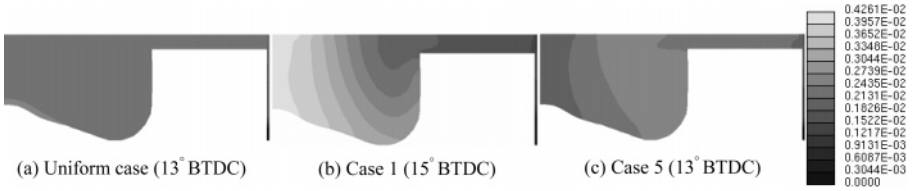

Figure 6. CH_2O concentration distributions of the uniform case, case 1, and case 5 when the high-temperature reactions are occurring ($\phi_{overall} = 0.264$).

Figure 7. In-cylinder temperature distributions of different imposed stratification cases when the high-temperature reactions are occurring ($\phi_{overall} = 0.264$).

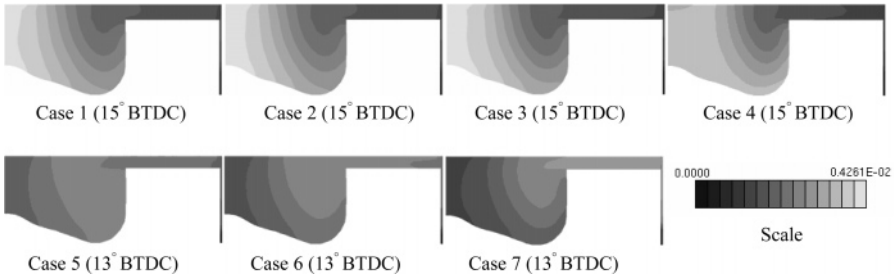

Figure 8. CH_2O concentration distributions of different imposed stratification cases when the high-temperature reactions are occurring ($\phi_{overall} = 0.264$).

CO emissions. The challenge for HCCI engines is to meet the control and high power output requirements of modern engines while keeping NOx and PM emissions low enough to meet current and future emissions standards. The effects of the seven kinds of stratification on emissions in the current study are analyzed in the following paragraphs.

A previous study found that UHC emissions of HCCI combustion mainly consist of unburned fuel and CH_2O.[35] Therefore, unburned fuel and CH_2O emissions are used to denote UHC emissions in the current study. Figures 9 and 10 show the comparison of unburned fuel, CH_2O, CO, and NOx emissions achieved from the uniform case and the seven kinds of stratification cases at two different overall equivalence ratios. In these two figures, the dashed line indicates the emissions of the uniform case; the mole percentage of fuel carbon into emissions is used to represent the values of unburned fuel, CH_2O, and CO emissions; The total grams of NOx emissions produced from the burning of every kilogram of fuel is used to denote the value of NOx emissions. Parts a and b of Figure 9 show that all seven kinds of stratification can reduce unburned fuel and CH_2O emissions at an overall equivalence ratio of 0.2. While, parts c and d of Figure 9 show that the former five kinds of stratification increase the CO emissions and the former four kinds of stratification increase the NOx emissions at an overall equivalence ratio of 0.2. Figure 10 shows that, at an overall equivalence ratio of 0.264, all seven kinds of stratification can reduce unburned fuel emissions; the former five kinds of stratification increase the CH_2O emissions and CO emissions; the former four kinds of stratification increase the NOx emissions. From the above analysis, it can be concluded that cases 6 and 7 can reduce UHC emissions and CO emissions simultaneously while NOx emissions hardly change. That is to say, a larger r/r_0 ratio has the potential of reducing UHC and CO emissions.

The average in-cylinder pressure analysis indicates that the former four kinds of stratification can reduce the pressure rise

(34) Fayoux, A.; Dupré, S.; Scouflaire, P.; Houille, S.; Pajot, O.; Rolon, C. OH and HCHO LIF Measurements in HCCI Engine. 12th International Symposium on Application of Laser Techniques to Fluid Mechanics, Lisbon, Portugal, Jul. 12−15, 2004.

(35) Yao, M. F.; Huang C.; Zheng, Z. L. Multi-dimensional Numerical Simulation on Dimethyl Ether/Methanol Dual Fuel HCCI Engine Combustion and Emission Processes. *Energy Fuels* **2007**, *21*, 812−821.

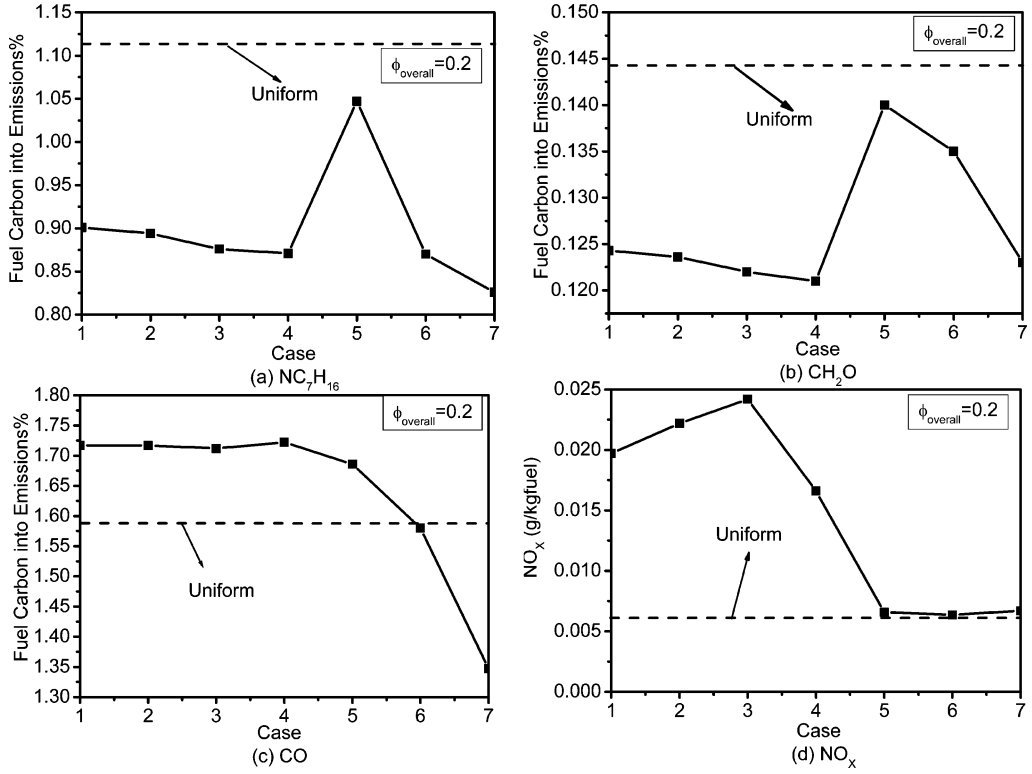

Figure 9. Comparison of UHC, CO, and NO_X emissions between seven kinds of stratification and the uniform case ($\phi_{overall} = 0.2$).

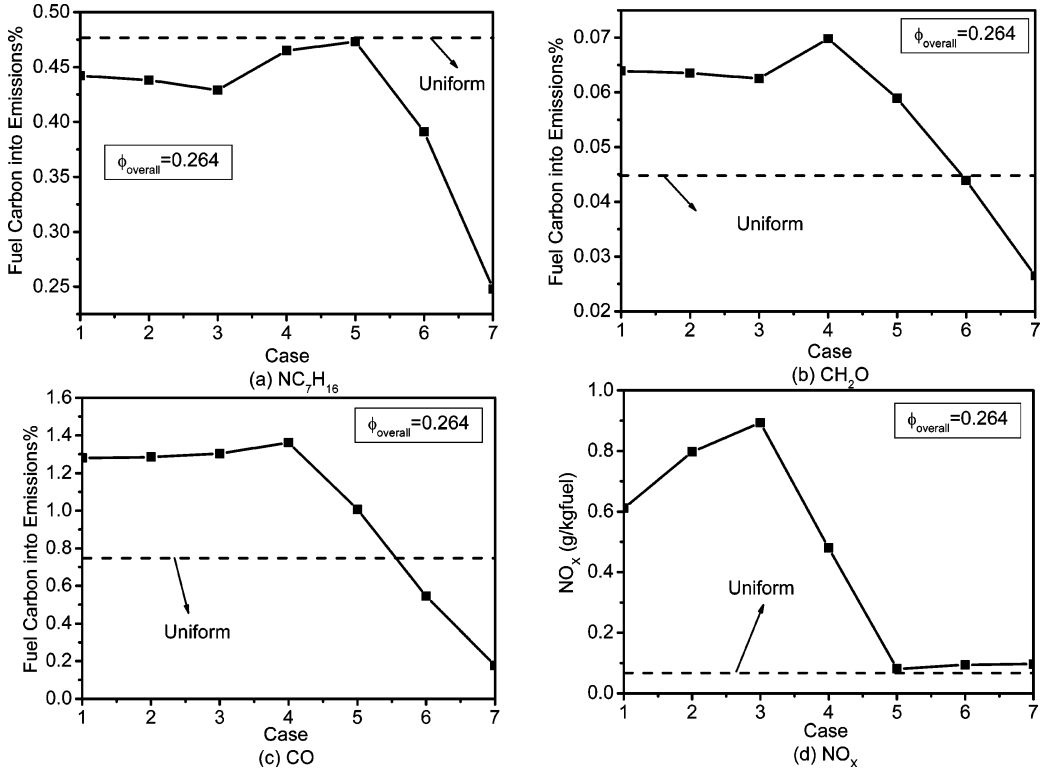

Figure 10. Comparison of UHC, CO, and NO_X emissions between seven kinds of stratification and the uniform case ($\phi_{overall} = 0.264$).

rate, but for emissions, all of them lead to an increase of CO and NOx emissions. It is the last two kinds of stratification that have the advantage of reducing emissions. Cases 1 and 6 with an overall equivalence ratio of 0.264 are selected as representatives to analyze the effects of stratification on the emissions.

Figures 11−13 show the concentration distributions of NC_7H_{16}, CH_2O, and CO at the end of the high-temperature reactions for the uniform case, case 6, and case 1, respectively. Figure 14 shows the in-cylinder temperature distributions of the three cases at the end of the high-temperature reactions. Figure 11 shows that fuel, CH_2O, and CO in the cylinder are oxidized completely at the end of high-temperature reactions for the uniform case. However, a small amount of the three species is left in the piston-ring crevice regions because the strong heat-transfer results in a low temperature here as shown in Figure 14a. Therefore, for HCCI combustion, UHC and CO emissions

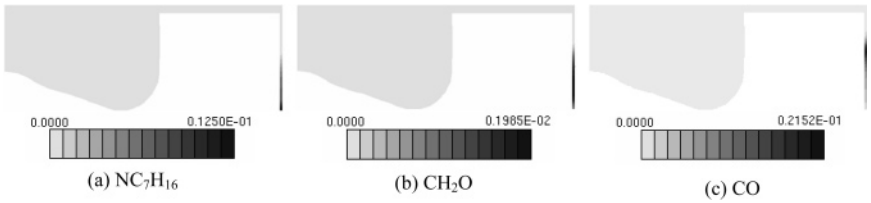

Figure 11. Concentration distributions of NC_7H_{16}, CH_2O, and CO for the uniform case at the end of the high-temperature reaction ($\phi_{overall}$ = 0.264).

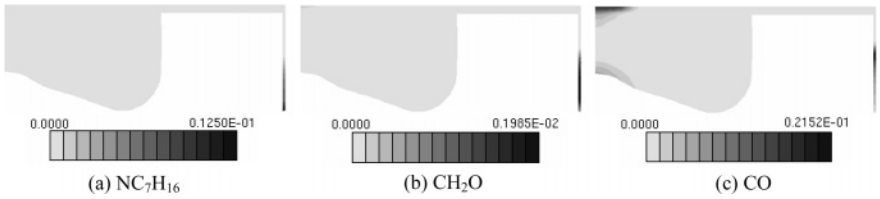

Figure 12. Concentration distributions of NC_7H_{16}, CH_2O, and CO for case 6 at the end of the high-temperature reaction ($\phi_{overall}$ = 0.264).

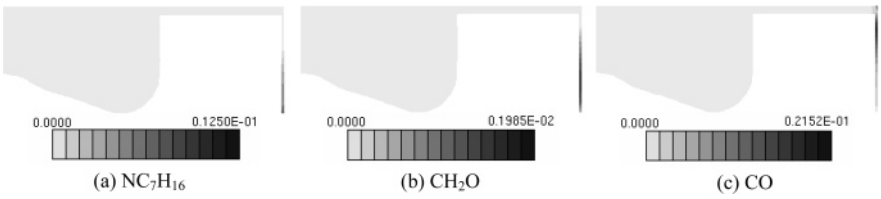

Figure 13. Concentration distributions of NC_7H_{16}, CH_2O, and CO for case 1 at the end of the high-temperature reaction ($\phi_{overall}$ = 0.264).

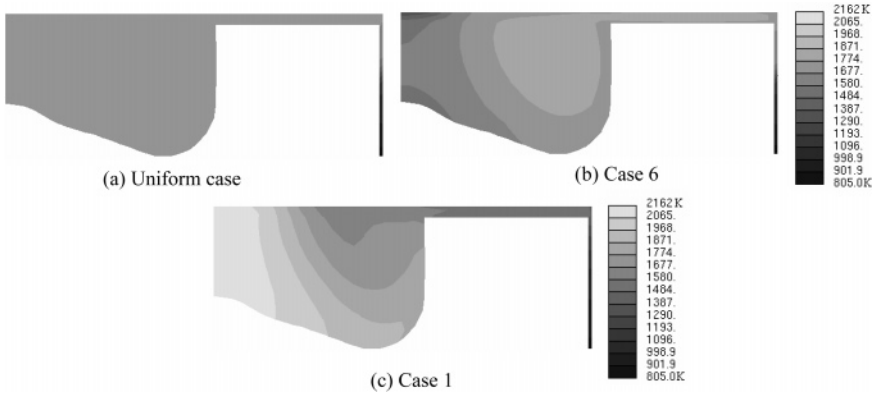

Figure 14. In-cylinder temperature distributions of the uniform case, case 1, and case 6 at the end of the high-temperature reaction ($\phi_{overall}$ = 0.264).

are mainly from the piston-ring crevice regions and are distributed near the cylinder liner wall with the piston moving down.

For the seven kinds of stratification in the current study, the fuel in the piston-ring crevice regions by initiation is less than that of the uniform case as shown in Table 1. Therefore, all kinds of stratification can reduce the unburned fuel emissions at two overall equivalence ratios. As shown in Figures 12a and 13a, the concentrations of unburned fuel for cases 1 and 6 are less than that of the uniform case at the end of the high-temperature reactions. In addition, Figures 9a and 10a also show that the unburned fuel emissions of case 5 are more than those of other cases. This is because, although the fuel in the piston-ring crevice regions for case 5 by initiation is less than that at the uniform case, it is more than that at other cases.

From a previous chemical kinetics analysis,[36] it can be known that most CH_2O is oxidized to HCO radicals by OH radicals in the process of hydrocarbon oxidation, while OH radicals are mainly produced by the decomposition of H_2O_2 only when the in-cylinder temperature is over 1000 K. If the fuel concentration and heat transfer of the piston-ring crevice regions lead to a wide temperature distribution range below 1000 K, a large amount of CH_2O cannot be oxidized and CH_2O emissions increase. The former five kinds of stratification at an overall equivalence ratio of 0.264 belong to this condition. For an example of case 1, stratification leads to a lean mixture in the piston-ring crevice regions, so the temperature distribution range below 1000 K extends compared with the uniform case as shown in Figure 14c. Consequently, a large amount of CH_2O cannot be oxidized in the piston-ring crevice regions. Figure 13b shows that the CH_2O concentration region in the piston-ring crevice regions for case 1 is much larger than that for case 6 and the uniform case at the end of the high-temperature reactions. Therefore, CH_2O emissions increase for case 1, though the highest concentration value is smaller than that for the uniform case. For case 6, both the temperature distribution range over 1000 K in the piston-ring crevice regions and the highest CH_2O concentration value are close to those for the uniform case at the end of the high-temperature reactions, so CH_2O emissions

(36) Yao, M. F.; Zheng, Z. L. Numerical Study on the Chemical Reaction Kinetics of n-Heptane for HCCI Combustion Process. *Fuel* **2006**, *85*, 2605−2615.

for case 6 are similar to those for the uniform case. With the maximal local equivalence ratio moving toward the cylinder wall (case 7), CH_2O emissions continue to decrease to the emission level below the threshold of the uniform case. At an overall equivalence ratio of 0.2, all kinds of stratification can reduce the CH_2O emissions because the lean mixture itself and the stratification lead to little fuel in the piston-ring crevice regions. Furthermore, the fuel in the piston-ring crevice regions for case 5 is the most in all stratified cases, so CH_2O emissions for case 5 are more than those for the other stratified cases.

In the oxidation of *n*-heptane, most CO is oxidized to CO_2 by OH radicals at the second stage of the high-temperature reaction. At this stage, the OH radical is mainly from the reaction $H + O_2 = OH + O$, which occurs only when the in-cylinder temperature is over 1400 K. At the two overall equivalence ratios in the current study, cases 6 and 7 can reduce CO emissions. The maximal local equivalence ratio appears at an r/r_0 ratio of 0.78 for case 6, and Figure 14b shows that the in-cylinder temperature near the maximal local equivalence ratio region for case 6 is higher than that of the same region for the uniform case. The temperatures in the regions at the top of the piston-ring crevice and near the cylinder wall are higher for case 6 than for the uniform case because the maximal local equivalence ratio region is located near these two strong heat-transfer regions for case 6. Consequently, the temperature regions below 1400 K in the piston-ring crevice regions are diminished and CO emissions decrease for case 6. Compared with Figures 11c and 12c, though the highest concentration value of CO for case 6 is higher than that for the uniform case at the end of the high-temperature reactions, the CO emissions still decrease because the high-concentration region is very small. In addition, for case 6, a small amount of CO is left in the regions of the cylinder head and the bottom of the combustion chamber near the cylinder centerline. This is because a very lean mixture in the regions near the cylinder centerline by this kind of stratification leads to comparatively low temperatures in the regions as shown in Figure 14b. For case 1, the mixture is too lean in the strong heat-transfer regions (the piston-ring crevice regions and the regions near the cylinder wall). Therefore, the temperatures in the whole piston-ring crevice regions are obviously below 1400 K. Consequently, a large amount of CO is left in the piston-ring crevice regions, and CO emissions for case 1 are higher than those for the uniform case.

NOx formation in engines occurs primarily through the high-temperature Zeldovich NOx formation mechanism,[37] which does not produce significant NOx until the temperature exceeds approximately 1900 K. At temperatures higher than 1900 K, the Zeldovich mechanism results in an exponential increase in NOx formation. Figure 14 shows that the highest in-cylinder temperature reaches 2162 K at the end of the high-temperature reactions for case 1; however, both for case 6 and for the uniform case, it is below 1900 K. Therefore, NOx emissions increase for case 1 but almost do not change for case 6.

(37) Warnatz, J.; Mass, U.; Dibble, R. W. Modeling and Simulation, Experiments, Pollutant Formation. *Combustion: Physical and Chemical Fundamentals*, 3rd ed.; Springer: Berlin, 2001.

4. Conclusions

In the current study, a fully coupled multidimensional CFD and reduced chemical kinetics model is adopted to investigate the combustion and emission processes of charge stratification. Seven different kinds of imposed theoretical stratification were introduced according to the position of the maximal local fuel/air equivalence ratio in the cylinder at intake valve close. The results can be summarized as follows:

At the two overall equivalence ratios in the current study which represent a leaner mixture and a comparatively richer mixture in HCCI combustion, the former four kinds of stratification, whose maximal local equivalence ratios locate in the range between the cylinder center and half of the cylinder radius at intake valve close, advance ignition timing and reduce the pressure-rise rate, but the other cases, whose the maximal local equivalence ratio appears between half of the cylinder radius and the cylinder wall at intake valve close, have no obvious effects on the average in-cylinder pressure.

All seven kinds of stratification can reduce unburned fuel emissions at the two overall equivalence ratios. When the mixture is leaner, all seven kinds of stratification can reduce CH_2O emissions; when the mixture is richer, only the last three kinds of stratification can reduce CH_2O emissions.

The former five kinds of stratification lead to the increase of CO emissions, and the former four kinds of stratification deteriorate NOx emissions. Only the last two kinds of stratification can reduce unburned fuel emissions, CH_2O emissions, and CO emissions simultaneously, while NOx emissions almost do not change.

Charge-stratified combustion has the potential of overcoming the problems of HCCI combustion (too rapid combustion, high CO emissions, and high UHC emissions).

Nomenclature

HCCI = homogenous charge compression ignition
UHC = unburned hydrocarbon
CO = carbon monoxide
CFD = computational fluid mechanics
IVC = intake valve close

Acknowledgment. The research is supported by the National Natural Science Found of China (NSFC) through its project (50676066).

EF070071K